

Path-conditioned Reinforcement Learning-based Local Planning for Long-Range Navigation

Mateo Haro, Julia Richter, Fan Yang, Cesar Cadena, Marco Hutter

Abstract—Long-range navigation is commonly addressed through hierarchical pipelines in which a global planner generates a path, decomposed into waypoints, and followed sequentially by a local planner. These systems are sensitive to global path quality, as inaccurate remote sensing data can result in locally infeasible waypoints, which degrade local execution. At the same time, the limited global context available to the local planner hinders long-range efficiency. To address this issue, we propose a reinforcement learning-based local navigation policy that leverages path information as contextual guidance. The policy is conditioned on reference path observations and trained with a reward function mainly based on goal-reaching objectives, without any explicit path-following reward. Through this implicit conditioning, the policy learns to opportunistically exploit path information while remaining robust to misleading or degraded guidance. Experimental results show that the proposed approach significantly improves navigation efficiency when high-quality paths are available and maintains baseline-level performance when path observations are severely degraded or even non-existent. These properties make the method particularly well-suited for long-range navigation scenarios in which high-level plans are approximate and local execution must remain adaptive to uncertainty.

Index Terms—Autonomous Navigation, Reinforcement Learning, Path-Aware Navigation, Mobile Robots

I. INTRODUCTION

Autonomous navigation is a fundamental capability of robotic systems and has become increasingly important as robots are deployed with higher levels of autonomy in complex, real-world environments. While planning and navigation have a long-standing history in robotics, the field has been profoundly reshaped in recent years by advances in deep learning and reinforcement learning (RL) [1]–[3]. Learning-based navigation systems offer improved robustness to uncertainty, partial observability, and sensor noise, and demonstrate strong generalization to dynamic and previously unseen environments [4]–[7]. These properties make RL particularly attractive for long-range navigation, where explicit maps may be unavailable or inaccurate. However, despite this progress, enabling RL agents to scale efficiently to long-horizon navigation tasks remains a central challenge, as pure goal-oriented exploration often leads to inefficient trajectories and poor utilization of available high-level information [7], [8].

Most navigation systems are structured hierarchically, decomposing the task into a high-level global planner and a low-level local planner [8]–[10]. The global planner is typically

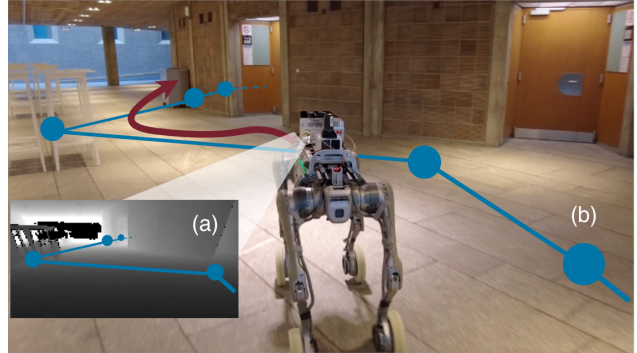


Fig. 1: The proposed path-aware local planner utilizes a reference path (b) to provide contextual guidance, augmenting depth camera observations (a) and proprioceptive feedback.

responsible for computing a path from the robot’s current location to the final goal, often based on coarse or incomplete map information, while the local planner executes short-range motions toward intermediate goals or waypoints. In many existing approaches, the global planner is typically assumed to provide an ideal and fully feasible path, and the local planner is often encouraged to follow this path as closely as possible [11], [12]. Other methods provide the local planner with only limited global context, such as a single waypoint [8], [10]. As a consequence, the local policy must rely heavily on exploration and reactive behaviors, which can lead to inefficiencies, repeated traversal of dead ends, and suboptimal long-range performance. In both cases, the local planner lacks a global understanding of the intended trajectory, either due to over-reliance on perfect guidance or insufficient access to global information [8]. While relatively few approaches provide local planners with rich global context without enforcing path adherence [5], [6], recent surveys such as [2] point to the integration of heuristic guidance into deep reinforcement learning (DRL) as a promising avenue for improving efficiency and long-range navigation performance.

In this work, we take a step in this direction by introducing a path-aware RL framework that incorporates coarse global path information as a form of heuristic guidance, without assuming this guidance is optimal or directly traversable. Rather than enforcing explicit path following, the policy learns to selectively exploit global path cues when they are informative and to disregard them when they are misleading, as illustrated in Fig. 1. We achieve this by extending a state-of-

All authors are with the Robotic Systems Lab (RSL), ETH Zürich, Zürich, Switzerland

Corresponding author: Mateo Haro, maharo@ethz.ch.

the-art RL-based navigation framework [7] with a structured path representation and a training procedure that integrates the global path information. In particular, we study how path information can be embedded and fused with perceptual observations, and how the training process can be designed to ensure that the policy uses this information selectively and robustly. Our core contributions are as follows:

- 1) **Path-conditioned navigation architecture:** We introduce a path-aware policy architecture that learns a structured representation of the global path and fuses it with perceptual observations.
- 2) **Path-conditioned training strategy:** We propose a training strategy that enables the policy to remain effective when path guidance is noisy or suboptimal.
- 3) **Real-world deployment:** We validate the proposed approach through various simulation experiments and real-world deployment, assessing architectural choices, training procedures, and robustness to noisy and suboptimal path observations.

The code is publicly released for the research community.

II. RELATED WORK

Historically, search-based algorithms, such as A* [13], have often been used alongside sampling-based methods [14], [15] to balance planning efficiency and exploration capabilities in discrete environments. The emergence of learning-based methods has further improved navigation capabilities by increasing adaptability to environmental uncertainty [5], [7], [16]. Many recent approaches integrate learned local planners alongside classical, non-learning-based global planners, reducing reliance on hand-crafted rules and extensive hyperparameter tuning [4], [16]. However, these systems still typically depend on explicit environment mapping, which comes with downsides as storage issues, dynamic obstacles, and a lack of map quality, as pointed out by [1].

In contrast to a hierarchical approach, several works have explored end-to-end DRL approaches for autonomous navigation in unknown environments [4], [17], [18]. These methods aim to remove explicit planning and mapping stages by learning reactive policies that map sensory inputs directly to control actions. While such approaches demonstrate strong autonomy and adaptability, multiple studies report reduced navigation efficiency due to the lack of global map information, often resulting in longer and more circuitous trajectories [17], [18].

Another line of research introduces plan- or path-conditioned reinforcement learning policies. These methods provide the agent with a reference trajectory and design reward structures that explicitly encourage adherence to the given path. The theory of plan-based shaping rewards [19] formalizes this approach and has been successfully applied theoretically [20], [21] as well as to autonomous driving, where precise path tracking is critical [12], [22]. However, such formulations inherently constrain the agent’s behavior, limiting its ability to explore or deviate from the reference path even when cheaper or safer alternatives exist.

The work most closely related to ours is L2E (Learn to Execute) [21], which proposes a plan-conditioned policy capable of reaching a goal even when the provided plan is partially incorrect. While L2E allows deviations when a plan becomes infeasible, its reward structure explicitly enforces proximity to the given trajectory whenever it is valid. Moreover, the approach is demonstrated primarily on manipulation tasks, which differ significantly from navigation in large-scale environments. In contrast, our approach does not aim to strictly execute a provided plan. Instead, we leverage the plan as contextual information while allowing the agent to opportunistically deviate whenever more efficient alternatives are observed, even if the original path remains feasible.

Overall, our work seeks to bridge pure goal-oriented exploration, DRL navigation, and path-conditioned control by combining the flexibility of learned policies with the guidance of a reference path, without explicitly enforcing path following, enabling a local planner that can be integrated into hierarchical navigation systems and intelligently exploit global planner path information.

III. PROBLEM FORMULATION

We consider the navigation problem introduced in [7], where an agent operates in an unknown 3D environment $E \subset \mathbb{R}^3$ and must reach a goal specified as a relative position $p_t \in \mathbb{R}^3$ to the agent’s egocentric frame at time step t , using only a single front-facing depth camera as exteroceptive input. The task is defined as reaching the goal region

$$\mathcal{G} = \{p_t \in \mathbb{R}^3 \mid \|p_t\| < \epsilon\} \quad (1)$$

within a maximum time horizon $t \leq T_{\max}$. Because the agent receives egocentric observations o_t that do not fully capture the underlying environment state s_t , the problem is formulated as a Partially Observable Markov Decision Process (POMDP) defined by the tuple $(\mathcal{S}, \mathcal{A}, \mathcal{T}, \mathcal{R}, \mathcal{O}, \mathcal{Z}, \gamma)$, where: \mathcal{S} is the environment state space, \mathcal{A} the agent action space, $\mathcal{T}(s, a, s')$ the transition probability function, $\mathcal{R}(s, a)$ the reward function, \mathcal{O} the agent observation space, $\mathcal{Z}(s, a, o)$ the observation probability function and $\gamma \in [0, 1]$ is the discount factor.

At each time step t , the agent receives an observation o_t and selects an action a_t according to a policy π . Since the state is not directly observable, the current observation is fused with the observation history $\mathcal{H}_{t-1} = \{o_1, \dots, o_{t-1}\}$ through a function f that produces a state estimate:

$$\hat{s}_t = f(o_t, \mathcal{H}_{t-1}). \quad (2)$$

The policy then computes the action

$$a_t = \pi(\hat{s}_t). \quad (3)$$

Both the state estimation function f and the policy π are jointly learned end-to-end via reinforcement learning, as described in the next section.

IV. METHODOLOGY

A. Path Representation and Encoding

Providing the full reference path allows the policy to reason over global structure, such as upcoming turns, large-scale deviations, or alternative routes, which cannot be captured by local look-ahead representations. Since our objective is to enable anticipatory behavior over long horizons, we encode the entire reference path rather than a truncated segment of arbitrary length, which would require task-specific tuning. Full-path observations offer a more general and robust representation, particularly in complex terrain and large-scale navigation scenarios. At time step t , the observation is defined as

$$o_t \in \mathcal{O}, \quad o_t = \{I_t, p_t, o_t^{prop}, \tilde{P}_t\}, \quad (4)$$

where I_t denotes the depth image, p_t the relative goal position, o_t^{prop} the proprioceptive observations, and \tilde{P}_t the relative reference path representation. The construction of \tilde{P}_t is described below. The reference path P_t is defined as a fixed-length sequence of N waypoints expressed in the robot's egocentric frame:

$$P_t = \{p_i\}_{i=1}^N, \quad p_i \in \mathbb{R}^3. \quad (5)$$

For each waypoint p_i , we compute its Euclidean distance to the robot:

$$d_i = \|p_i\|_2. \quad (6)$$

We then construct an augmented waypoint representation $\tilde{p}_i \in \mathbb{R}^4$ defined as

$$\tilde{p}_i = \begin{bmatrix} p_i \\ \frac{\max(d_i, \epsilon)}{\log(1 + d_i)} \\ c \end{bmatrix}, \quad (7)$$

where $\frac{p_i}{\max(d_i, \epsilon)}$ encodes the normalized direction of the waypoint, with ϵ a small constant preventing division by zero, and $\log(1 + d_i)$ compresses large distance variations. The constant $c = \max_i(\log(1 + d_i))$ denotes a normalization factor ensuring bounded inputs for training stability. The final path representation \tilde{P}_t encodes the waypoints' direction and log-distance to the current robot pose and is therefore

$$\tilde{P}_t = \{\tilde{p}_i\}_{i=1}^N, \quad \tilde{p}_i \in \mathbb{R}^4. \quad (8)$$

This relative encoding enables generalization across varying path lengths and geometries, while absolute distance information remains accessible through p_t . Note that p_t is not constrained to coincide with the final waypoint p_N , as the reference path may not necessarily align with the goal position, for example due to the noise introduced during training, as described in the following section.

To encode the path, we employ a combination of self-attention and cross-attention mechanisms, as illustrated in Fig. 2. Self-attention enables interaction among waypoints and captures global path structure, producing a compact set of informative features. While self-attention alone could serve as a dimensionality-reduction mechanism, we also introduce cross-attention to allow the policy to selectively focus on relevant segments of the path. Specifically, the cross-attention

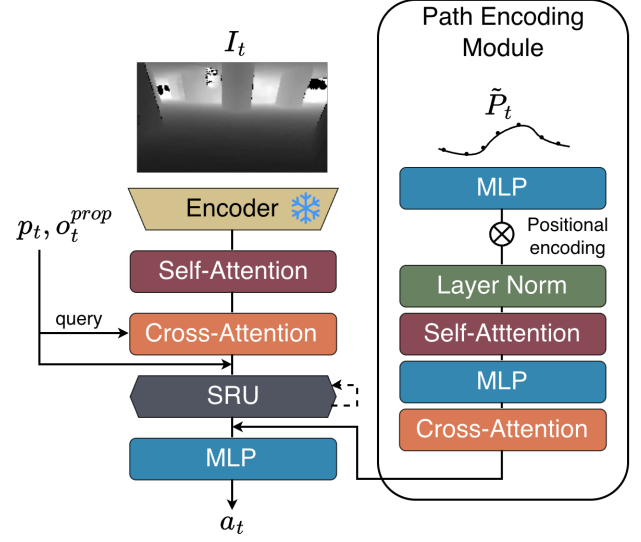


Fig. 2: Overview of the proposed path-aware navigation architecture. The base navigation pipeline, including the pretrained depth image encoder, the spatially-enhanced recurrent unit, the fusion of relative goal position p_t and proprioceptive observations o_t^{prop} with visual features, follows [7]. We extend this framework with the proposed Path Encoding module, enabling implicit conditioning on reference path information.

query is implemented as a learnable embedding of fixed dimension, enabling the model to attend to path regions that are most informative for the current navigation context, such as sharp turns or critical deviations. The resulting path embedding is concatenated with the output of the spatially-enhanced recurrent unit (SRU), as illustrated in Fig. 2. In contrast, proprioceptive features are integrated upstream of the SRU and contribute to its hidden state. This design reflects the assumption that the reference path remains fixed during an episode and therefore does not require temporal integration within the recurrent memory.

B. Training Path Generation

Rather than training exclusively on optimal trajectories, we sample reference paths from a controlled distribution that includes feasible but suboptimal solutions. This prevents the policy from collapsing to strict path-following behavior while preserving informative global guidance. To further increase robustness, we intentionally perturb paths with noise, which can make them locally infeasible.

Optimal reference paths are generated using A* search on a graph constructed via a Probabilistic Roadmap (PRM). To introduce controlled sub-optimality, we additionally employ Greedy Best-First Search (GBFS) with a biased heuristic that encourages detours. While the standard admissible A* heuristic corresponds to the Euclidean distance to the goal in 3D space, we modify it by incorporating an attraction term

toward a randomly sampled detour point p :

$$h = \beta d_g + (1 - \beta) d_p, \quad (9)$$

where d_g denotes the Euclidean distance to the goal, d_p the Euclidean distance to the detour point p , and $\beta \in [0, 1]$ controls the strength of the goal-directed bias. Lower values of β increase the influence of the detour term and increase sub-optimality.

During training, the reference path is randomly generated either using standard A* with the Euclidean heuristic or GBFS with the biased heuristic in (9). The sampling probability and the bias parameter β shape the distribution of reference paths and therefore influence the learning dynamics. For each episode, the resulting path is post-processed using a line-of-sight smoothing procedure. Additionally, random perturbations are independently applied to each waypoint to further increase variability. As a consequence, some reference paths may become partially infeasible due to collisions or constraint violations.

C. Reward Design for Opportunistic Deviation

The navigation objective is to reach the goal region as efficiently as possible. We adopt the reward formulation of [7] and summarize it here for completeness. The reward is purely goal-driven and contains no explicit path-following term. At each timestep t , the total reward is

$$r_t = \alpha_1 r_t^{\text{task}} + \alpha_2 r_t^{\text{reg}} + \alpha_3 r_t^{\text{pen}} + \alpha_4 r_t^{\text{shortcut}}, \quad (10)$$

where r_t^{task} promotes task completion, r_t^{reg} enforces motion smoothness, and r_t^{pen} penalizes unsafe behavior.

Task Reward:

$$r_t^{\text{task}} = \frac{\mathbf{1}(t > T_{\max} - T_r \vee \text{random} < \delta_{\text{check}})}{1 + \left\| \frac{p_t}{\sigma} \right\|_2}, \quad (11)$$

where p_t is the relative goal position, σ a normalization factor, T_{\max} the episode horizon, and T_r the terminal reward window.

Regularization:

$$r_t^{\text{reg}} = \beta_1 \|a_t - a_t^m\|_1 + \beta_2 \|j_t^{\text{acc}}\|_1, \quad (12)$$

where a_t denotes the executed action, j_t^{acc} the joint accelerations, and

$$a_t^m = \lambda a_{t-1}^m + (1 - \lambda) a_t \quad (13)$$

is a momentum-filtered action with factor λ .

Penalties:

$$r_t^{\text{pen}} = \eta_1 \mathbf{1}(\text{collision}) + \eta_2 \max(0, |\theta_t| - \theta_{\text{safe}}), \quad (14)$$

where θ_t is the body inclination and θ_{safe} a safety threshold. To encourage opportunistic deviation from suboptimal or noisy reference paths, we introduce an additional shortcut reward r_t^{shortcut} . A shortcut is identified when the agent’s progress along the reference path exceeds a threshold of the total path length within a single simulation timestep. When this condition is met, a positive reward is granted, explicitly reinforcing

behaviors that bypass unnecessary detours suggested by the reference path. Formally, the shortcut reward is defined as:

$$r_t^{\text{shortcut}} = \begin{cases} \Delta p, & \text{if } \Delta p > \epsilon \\ 0, & \text{if } \Delta p \leq \epsilon \end{cases} \quad (15)$$

It indicates whether a shortcut event occurred at timestep t , Δp denotes the progress in percent along the path between two consecutive time steps, ϵ denotes the threshold at which we consider a shortcut, and α_4 is a scalar weight controlling the influence of the shortcut reward.

To summarize, the reward structure depends exclusively on goal-reaching and stability objectives; any path-following behavior must therefore emerge implicitly from the observation-conditioning and training procedure. Finally, the policy is trained following an Asymmetric Actor-Critic PPO pipeline and with the training regularization techniques presented in [7], namely Temporally Consistent Dropout and Deep Mutual Learning.

V. EXPERIMENTS

A. Training and Simulation Details

The RL training, experiments, and simulation environment are implemented in Isaac Sim using Isaac Lab [23], [24] and the `rsl-rl` framework [25]. The final policy is trained entirely in simulation for 39.5 hours on a single NVIDIA GeForce RTX 4090, with 1046 agents simulated in parallel across 180 procedurally generated environments. No dedicated curriculum is employed; instead, domain randomization is applied to the policy inputs to enhance sim-to-real generalization. The proprioceptive observation o_t^{prop} consists of the linear and angular velocities (v_t, ω_t) as well as the projected gravity vector n_t . Additionally, the reference path \tilde{P}_t is composed of $N = 15$ waypoints. The simulated depth camera has a horizontal field of view of 105° , a vertical field of view of 78° , and a maximum sensing range of 10 m. The navigation policy operates at 5 Hz and outputs an action a_t , which is executed by a separate locomotion policy running at 50 Hz for low-level control.

B. Experimental Setup and Evaluation Metrics

After comparing the baseline policy against our final path-aware model in Section V-C, we conduct a set of experiments to validate the design choices introduced in Section IV. Section V-D1 assesses the impact of architectural decisions by comparing several variants of the path encoding module against each other. To enable a controlled comparison, the architectural variants are trained on an optimal reference path, allowing us to isolate the model’s ability to encode and exploit path information without confounding effects from path degradation. Secondly, Section V-D2 evaluates different training procedures. In this setting, all policies are tested using degraded reference paths that are both noisy and suboptimal, in order to assess their robustness to imperfect path guidance.

To perform the evaluations in Sections V-C–V-D2, we establish the following evaluation protocols and metrics. We

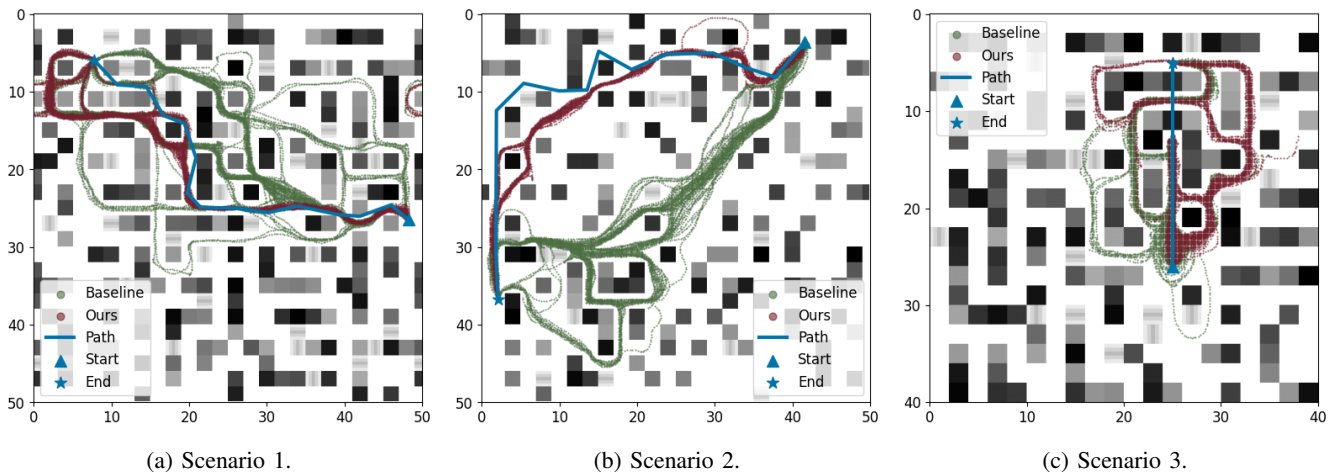


Fig. 3: Qualitative comparison of navigation trajectories in a 50×50 m and 40×40 m maze environments. For each policy, 100 trajectories are shown.

define evaluation conditions that differ from those encountered during training, in order to assess generalization. Specifically, while training is performed on environments of size 30×30 m, evaluation is conducted on larger terrains of size 50×50 m. The maximum episode duration is also increased from 60 s during training to 120 s at evaluation time. The procedural terrain generation process is kept identical, ensuring that obstacle distributions remain statistically consistent while increasing the spatial scale of the task. We evaluate all policies across 75 procedurally generated terrains, resulting in up to 2250 evaluation episodes (30 trajectories per terrain). When a testing episode is repeated, the starting position remains fixed while the robot’s initial orientation is randomized. Performance is quantified primarily using the Success Rate (SR) and the Success weighted by Path Length (SPL), described in [3] and defined as

$$\text{SPL} = \frac{1}{N} \sum_{i=1}^N S_i \frac{L_i}{\max(l_i, L_i)}, \quad (16)$$

where L_i is the optimal path length, computed using the A* with the standard Euclidean distance as a heuristic, and l_i is the robot’s trajectory length. To provide a more fine-grained analysis, the SPL is reported as a function of the optimal path length.

We establish two evaluation reference path scenarios: (1) the agent is provided with the optimal path computed by the planner, (2) the agent observes a degraded reference path that is both noisy and suboptimal. To assess robustness beyond training conditions, waypoint noise is sampled with a displacement magnitude ranging up to 2 m, compared to 1 m in training. In addition, non-optimal paths are selected so that their total length lies between 1.25 and 3.33 times that of the corresponding optimal path. This evaluation protocol allows us to assess both the best-case performance when high-quality path information is available and the worst-case behavior when reference paths are misleading or unreliable.

C. Comparison with Baseline Navigation

We compare our path-aware model against the baseline policy from [7] under the two reference path observation scenarios introduced in V-B. Table I summarizes the SR and SPL results for both policies. When provided with an optimal reference path, the path-aware model achieves a 7.02% increase in SPL compared to the baseline, demonstrating its ability to effectively exploit high-quality path information. Under degraded path observations, the performance of our model remains comparable to the baseline, indicating that misleading or unreliable path information does not degrade navigation performance. These results highlight that the proposed method improves navigation efficiency when informative path observations are available, while maintaining baseline-level performance when path information is poor or unreliable.

We also conduct qualitative experiments to analyze the behavior of the proposed path-aware policy compared to the baseline. As illustrated in Fig. 3, the path-aware model consistently exploits the provided path information to guide its exploration. Compared to the baseline, the resulting trajectories exhibit significantly lower variability and greater consistency across episodes. Even when the suggested path is suboptimal (b), the path-aware agent generally benefits from the high-level directional cues, leading to more efficient navigation and fewer unnecessary detours. Furthermore, it can still reach the goal when the reference path is blocked, and additional exploration is required (c). These qualitative results, together with the results from Table I, suggest that the proposed approach successfully induces the desired behavior, guiding exploration

TABLE I: Performance comparison between the baseline and our model.

| Model | SR | SPL |
|---------------------------------|-------------|-------------|
| Baseline | 0.83 | 0.75 |
| Our model (optimal path) | 0.87 | 0.82 |
| Our model (non-optimal & noisy) | 0.83 | 0.74 |

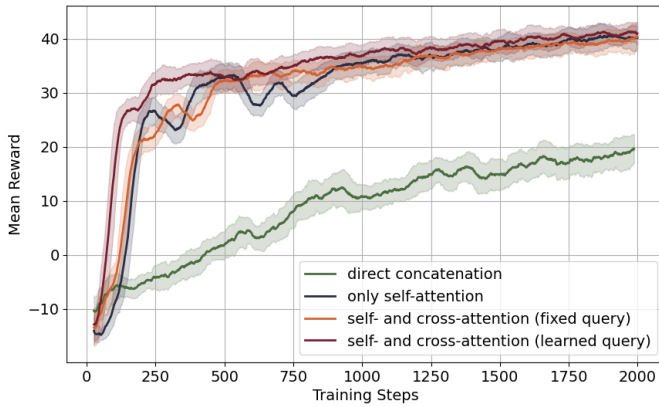


Fig. 4: Comparison of training reward across different path encoding architectures, illustrating the effect of architectural choices on learning performance.

while preserving the ability to deviate from imperfect guidance when beneficial.

D. Ablation Study

We now analyze which design choices contribute to this improvement.

1) *Model Architecture Ablation*: We first evaluate the capacity of the proposed architecture to exploit reference path information. To isolate this effect, we consider an idealized setting in which the observed path corresponds to the optimal trajectory computed by the global planner. This experiment is designed to assess whether the policy can leverage path information purely through its representation and integration within the network. We compare several variants of the path encoding module, differing in how the path representation is processed before being concatenated with the rest of the policy features:

- 1) direct concatenation of the raw path representation,
- 2) only self-attention-based path encoding,
- 3) self- and cross-attention with a fixed random query,
- 4) self- and cross-attention with a learned query.

As shown in Fig. 4, the learned-query variant exhibits the steepest initial slope of the learning curve, indicating the fastest rate of performance improvement during early training. It also maintains consistently higher rewards than the other variants over the first 2000 training iterations. We therefore adopted this variant for our final model and all subsequent experiments.

2) *Training Process Ablation*: We then evaluate the robustness of path-aware policy variants obtained from different training procedures using the SR and SPL metric with the considered policies specified in Table II. All models are evaluated under the poor path quality scenario defined in V-B. Table III summarizes the SR and SPL results across all ablations.

The results indicate that models trained without waypoint noise exhibit significantly reduced robustness when evaluated on degraded path observations. While all path-aware

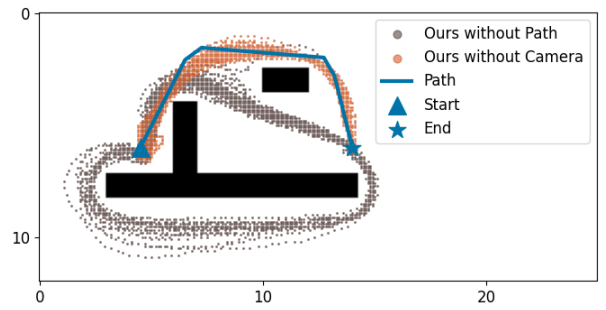


Fig. 5: Qualitative comparison of a 100 navigation trajectories under input ablation, where the scale is in meters.

variants outperform rigid path-following behavior, the full model achieves the highest average SR. Although the overall performance gap between the full model and the shortcut-reward ablated variant is modest, the full model exhibits significantly less degradation on longer trajectories.

E. Robustness to Missing Inputs

We evaluate the robustness of the policy to missing inputs by simulating extreme sensing conditions in which specific input modalities are replaced with zero tensors, as illustrated in Fig. 5. Two scenarios are considered: (1) removing the reference path observation and (2) removing the depth image input. When the reference path is ablated, the agent behaves similarly to the baseline, reaching the goal through unguided exploration even in larger 50×50 m environments. This indicates that the policy can rely solely on perceptual inputs when path information is unavailable. Conversely, when the depth input is removed, the agent exhibits path-following behavior, navigating primarily based on the waypoint sequence. Although successful execution is mainly observed for shorter, less perturbed paths, this demonstrates that the model can effectively interpret and exploit structured path information in the absence of visual input.

F. Real-world Test

To further assess the robustness and transferability of our approach, we deployed the trained policy on a Unitree B2W quadruped in a previously unseen indoor environment. The robot is equipped with a ZEDX depth camera and an NVIDIA Jetson AGX Orin for onboard computation. Proprioceptive observations σ_t^{prop} are provided by a LiDAR-based state estimation system.

TABLE II: Training configuration and ablation settings.

| Model | Sub-optimal Path | Path Noise | Shortcut Reward |
|-------------------------|------------------|------------|-----------------|
| Path Follower | no | no | no |
| Reward & Noise Ablation | yes | no | no |
| Reward Ablation | yes | yes | no |
| Noise Ablation | yes | no | yes |
| Full Model | yes | yes | yes |

TABLE III: SR and SPL as a function of optimal path length.

| Model | 0-10m | | 10-20m | | 20-30m | | 30-40m | | 40-50m | | 50-60m | | 60-70m | |
|-------------------------|-------------|-------------|-------------|-------------|-------------|-------------|-------------|-------------|-------------|-------------|-------------|-------------|-------------|-------------|
| | SPL | SR |
| Path follower | 0.39 | 0.63 | 0.24 | 0.40 | 0.19 | 0.32 | 0.15 | 0.25 | 0.13 | 0.19 | 0.07 | 0.09 | 0.04 | 0.05 |
| Reward & Noise Ablation | 0.43 | 0.54 | 0.38 | 0.45 | 0.34 | 0.39 | 0.35 | 0.41 | 0.38 | 0.45 | 0.31 | 0.38 | 0.26 | 0.28 |
| Full Model | 0.79 | 0.89 | 0.82 | 0.89 | 0.80 | 0.88 | 0.74 | 0.82 | 0.71 | 0.82 | 0.62 | 0.71 | 0.63 | 0.70 |
| Reward Ablation | 0.83 | 0.92 | 0.84 | 0.91 | 0.81 | 0.87 | 0.75 | 0.82 | 0.72 | 0.82 | 0.62 | 0.69 | 0.50 | 0.54 |
| Noise Ablation | 0.22 | 0.29 | 0.21 | 0.25 | 0.19 | 0.23 | 0.21 | 0.24 | 0.18 | 0.22 | 0.12 | 0.14 | 0.15 | 0.18 |

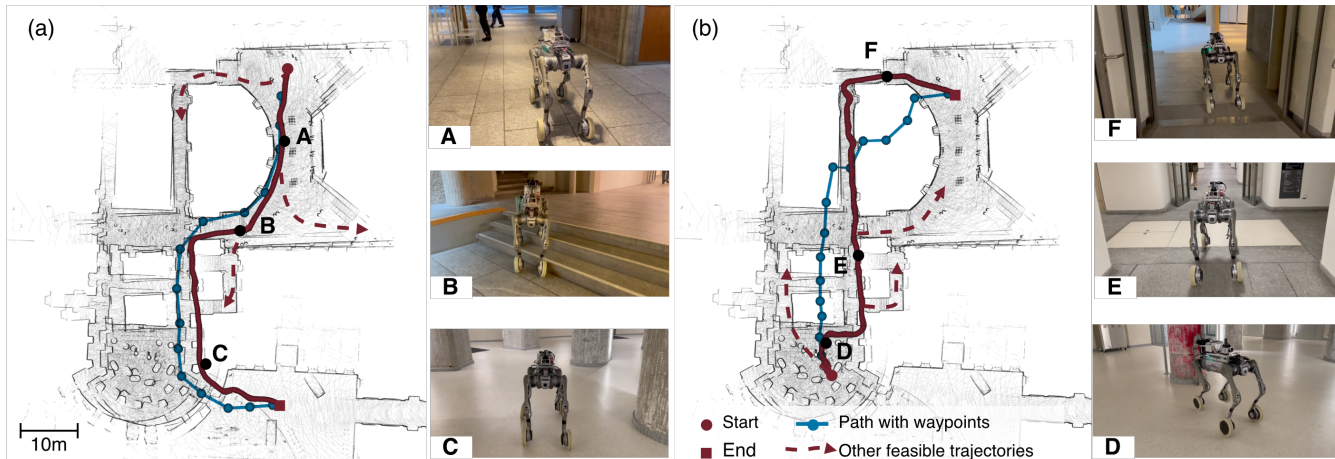


Fig. 6: Real-world deployment in a university building with long-range navigation trajectories. The robot trajectory shown by the continuous red line spans about 93 m in scenario (a) and 91 m in scenario (b).

As illustrated in Fig. 6, the real-world results are consistent with the behaviors observed in simulation, particularly in long-range navigation scenarios involving extended traversals and multiple directional commitments. Importantly, the reference path is intentionally selected to reduce stair traversal rather than to minimize distance. Even when the provided path is imperfect, the policy leverages it to bias exploration and avoids entering corridors that would yield trajectories of comparable length but increased uncertainty. More specifically, the dashed red arrows indicate alternative routes that would have reached the goal with similar path length but required negotiating more stairs, resulting in less reliable and less safe terrain for the locomotion policy; some alternatives also lead to dead ends or longer detours. Together, these experiments demonstrate successful sim-to-real transfer and highlight the model’s capacity to integrate global path information with local perception, biasing the robot toward safer and more desirable trajectories while preserving goal-reaching performance.

VI. DISCUSSION

A. Opportunistic Use of Path Information

We observe that training with exclusively optimal reference paths promotes rigid path-following behavior, whereas exposure to imperfect or infeasible paths encourages the policy to learn when and how to trust path information. Consistent with this, the experimental results indicate that the proposed model exploits path guidance opportunistically rather than blindly following it. When the reference path is near-optimal

and reliable, the policy improves navigation efficiency by reducing unnecessary exploration, dead ends, and detours. Conversely, when the path is misleading or suboptimal, the agent prioritizes goal-directed reasoning over strict adherence to the provided guidance.

This behavior can be attributed to the combination of implicit path conditioning and the underlying reward structure. Although the model is trained on suboptimal, noisy paths, the reward function remains focused on reaching the goal efficiently, without explicitly rewarding path-following. As a result, the policy is encouraged to treat the path as contextual guidance rather than as an execution constraint. Implicit conditioning, therefore, enables the model to modulate its behavior based on the observed path while preserving its fundamental objective of reaching the goal as efficiently as possible.

B. Fixed Path Representation

The current model represents the reference path using a fixed number of waypoints, which limits the number of turns and the spatial extent it can represent. While this choice is sufficient for the environments’ size considered in this work, it may restrict scalability to longer-range navigation scenarios spanning hundreds of meters. Future work could investigate the impact of increasing the waypoint count or, more generally, develop architectures capable of processing paths with a variable number of waypoints.

C. Implicit Modeling of Path Reliability

The policy implicitly learns how much to rely on the reference path through exposure to suboptimal and noisy paths during training. While this enables opportunistic use of path information, it also introduces two limitations. First, the resulting behavior depends strongly on the training path distribution, making it difficult to precisely tune or predict the learned reliance on path information. Second, at inference time, the policy treats all observed paths uniformly and cannot explicitly distinguish between accurate and unreliable guidance.

A natural extension would be to incorporate explicit reasoning about path quality. Path reliability could be provided as an additional observation by a high-level planner or estimated online by the policy itself. For instance, path features could be gated by the SRU's internal state, which encodes the agent's recent experience and interaction history. Such a mechanism would allow the policy to dynamically modulate its reliance on the reference path.

VII. CONCLUSION

We proposed a path-aware local navigation policy that leverages reference path information opportunistically rather than treating it as an explicit execution constraint. By conditioning an RL policy on imperfect and potentially misleading path observations, our approach addresses key limitations of purely exploratory, goal-oriented navigation, such as unnecessary detours and dead-end exploration.

Our experimental results demonstrate that access to path information significantly improves navigation efficiency when high-quality paths are available, while performance gracefully degrades to baseline levels when path observations are severely degraded. This behavior highlights the robustness of implicit path conditioning and distinguishes it from rigid path-following approaches. The proposed method is particularly well-suited for long-range navigation scenarios in which high-level planning is inaccurate, but local execution must remain adaptive to uncertainty and environmental variability.

ACKNOWLEDGMENT

This research was supported by the Swiss National Science Foundation (SNSF) as part of project No.227617.

REFERENCES

- [1] S. Nahavandi, R. Alizadehsani, D. Nahavandi, S. Mohamed, N. Mohajer, M. Rokonzaman, and I. Hossain, "A comprehensive review on autonomous navigation," *ACM Comput. Surv.*, vol. 57, no. 9, May 2025. [Online]. Available: <https://doi.org/10.1145/3727642>
- [2] T. T. Nguyen, S. Nahavandi, I. Razzak, D. Nguyen, N. T. Pham, and Q. V. H. Nguyen, "The emergence of deep reinforcement learning for path planning," 2025. [Online]. Available: <https://arxiv.org/abs/2507.15469>
- [3] P. Anderson, A. Chang, D. S. Chaplot, A. Dosovitskiy, S. Gupta, V. Koltun, J. Kosecka, J. Malik, R. Mottaghi, M. Savva *et al.*, "On evaluation of embodied navigation agents," 2018. [Online]. Available: <https://arxiv.org/abs/1807.06757>
- [4] T. Fan, X. Cheng, J. Pan, D. Manocha, and R. Yang, "Crowdmov: Autonomous mapless navigation in crowded scenarios," *arXiv preprint arXiv:1807.07870*, 2018.
- [5] D. Shah and S. Levine, "ViKiNG: Vision-Based Kilometer-Scale Navigation with Geographic Hints," in *Proceedings of Robotics: Science and Systems*, 2022. [Online]. Available: <http://www.roboticsproceedings.org/rsss18/p019.html>
- [6] J. Truong, A. Zitkovich, S. Chernova, D. Batra, T. Zhang, J. Tan, and W. Yu, "Indoorsim-to-outdoorreal: Learning to navigate outdoors without any outdoor experience," *IEEE Robotics and Automation Letters*, vol. 9, no. 5, pp. 4798–4805, 2024.
- [7] F. Yang, P. Frivik, D. Hoeller, C. Wang, C. Cadena, and M. Hutter, "Spatially-enhanced recurrent memory for long-range mapless navigation via end-to-end reinforcement learning," *International Journal of Robotics Research*, 2025.
- [8] J. Richter, T. Tuna, M. Patel, T. Miki, D. Higgins, J. Fox, C. Cadena, A. Diaz, and M. Hutter, "Large-scale autonomous gas monitoring for volcanic environments: A legged robot on mount etna," *arXiv preprint arXiv:2601.07362*, 2026.
- [9] R. Siegwart and I. R. Nourbakhsh, *Introduction to autonomous mobile robots / Roland Siegwart and Illah R. Nourbakhsh.*, ser. Intelligent robots and autonomous agents. Cambridge, Mass. : MIT Press, 2004.
- [10] M. Mattamala, N. Chebrolu, B. Casseau, L. Freißmuth, J. Frey, T. Tuna, M. Hutter, and M. Fallon, "Autonomous forest inventory with legged robots: system design and field deployment," *arXiv preprint arXiv:2404.14157*, 2024.
- [11] M. Hentschel and B. Wagner, "Autonomous robot navigation based on openstreetmap geodata," in *13th International IEEE Conference on Intelligent Transportation Systems*. IEEE, 2010, pp. 1645–1650.
- [12] X. Cheng, S. Zhang, S. Cheng, Q. Xia, and J. Zhang, "Path-following and obstacle avoidance control of nonholonomic wheeled mobile robot based on deep reinforcement learning," *Applied Sciences*, vol. 12, no. 14, 2022. [Online]. Available: <https://www.mdpi.com/2076-3417/12/14/6874>
- [13] P. Hart, N. Nilsson, and B. Raphael, "A formal basis for the heuristic determination of minimum cost paths," *IEEE Transactions on Systems Science and Cybernetics*, vol. 4, no. 2, pp. 100–107, 1968. [Online]. Available: <https://doi.org/10.1109/tssc.1968.300136>
- [14] S. M. LaValle, "Rapidly-exploring random trees : a new tool for path planning," *The annual research report*, 1998. [Online]. Available: <https://api.semanticscholar.org/CorpusID:14744621>
- [15] L. E. Kavradi, P. Svestka, J.-C. Latombe, and M. H. Overmars, "Probabilistic roadmaps for path planning in high-dimensional configuration spaces," *IEEE transactions on Robotics and Automation*, vol. 12, no. 4, pp. 566–580, 2002.
- [16] J. Lee, M. Bjelonic, A. Reske, L. Wellhausen, T. Miki, and M. Hutter, "Learning robust autonomous navigation and locomotion for wheeled-legged robots," *Science Robotics*, vol. 9, no. 89, Apr. 2024. [Online]. Available: <http://dx.doi.org/10.1126/scirobotics.ad9641>
- [17] H. Shi, L. Shi, M. Xu, and K.-S. Hwang, "End-to-end navigation strategy with deep reinforcement learning for mobile robots," *IEEE Transactions on Industrial Informatics*, vol. 16, no. 4, pp. 2393–2402, 2019.
- [18] R. Cimurs, I. H. Suh, and J. H. Lee, "Goal-driven autonomous exploration through deep reinforcement learning," *IEEE Robotics and Automation Letters*, vol. 7, no. 2, pp. 730–737, 2021.
- [19] I. Schubert, O. S. Oguz, and M. Toussaint, "Plan-based relaxed reward shaping for goal-directed tasks," *arXiv preprint arXiv:2107.06661*, 2021.
- [20] B. Wang, Z. Liu, Q. Li, and A. Prorok, "Mobile robot path planning in dynamic environments through globally guided reinforcement learning," *IEEE Robotics and Automation Letters*, vol. 5, no. 4, pp. 6932–6939, 2020.
- [21] I. Schubert, D. Driess, O. S. Oguz, and M. Toussaint, "Learning to execute: Efficient learning of universal plan-conditioned policies in robotics," *Advances in Neural Information Processing Systems*, vol. 34, pp. 1912–1924, 2021.
- [22] H. Merton, T. Delamore, K. Stol, and H. Williams, "Deep reinforcement learning for local path following of an autonomous formula sae vehicle," *arXiv preprint arXiv:2401.02903*, 2024.
- [23] M. Mittal, C. Yu, Q. Yu, J. Liu, N. Rudin, D. Hoeller, J. L. Yuan, R. Singh, Y. Guo, H. Mazhar *et al.*, "Orbit: A unified simulation framework for interactive robot learning environments," *IEEE Robotics and Automation Letters*, vol. 8, no. 6, pp. 3740–3747, 2023.
- [24] M. Mittal, P. Roth, J. Tigue, A. Richard, O. Zhang, P. Du, A. Serrano-Muñoz, X. Yao, R. Zurbrügg, N. Rudin *et al.*, "Isaac lab: A gpu-accelerated simulation framework for multi-modal robot learning," *arXiv preprint arXiv:2511.04831*, 2025. [Online]. Available: <https://arxiv.org/abs/2511.04831>

- [25] C. Schwarke, M. Mittal, N. Rudin, D. Hoeller, and M. Hutter, "Rsl-rl: A learning library for robotics research," *arXiv preprint arXiv:2509.10771*, 2025.